A VERY-HIGH-ENERGY NEUTRINO TELESCOPE ON-BOARD EUSO-SPB2 MISSION*

Mahdi Bagheri, Eliza Gazda, Oscar Romero Matamala
A. Nepomuk Otte

School of Physics and Center for Relativistic Astrophysics
Georgia Institute of Technology, 837 State Street NW, Atlanta, GA 30332, USA

Eleanor G. Judd

Space Sciences Laboratory, University of California, Berkeley, CA 94720, USA

Evgeny N. Kuznetsov, Patrick J. Reardon

The University of Alabama in Huntsville, Huntsville, AL 35899, USA

Michael J. Miller, Yaser Onel

The University of Iowa, Iowa City, IA 52242, USA

on behalf of the JEM-EUSO Collaboration

Received 15 April 2022, accepted 4 May 2022,
published online 9 September 2022

We present the status of the development of a Cherenkov telescope onboard the Extreme Universe Space Observatory Super Pressure Balloon 2 (EUSO-SPB2). EUSO-SPB2 is an approved NASA balloon mission that is planned to fly in 2023 from Wanaka, NZ and is a pathfinder for future space-based missions to detect astrophysical neutrinos. The objectives of this mission are to classify the sources of background and make the first observation of Very-High-Energy (VHE) cosmic rays via Cherenkov technique from suborbital altitude. We also intend to perform target of opportunity searches in response to multi-messenger alerts and use the Earth-skimming technique to search for VHE-tau neutrinos below the Earth's limb ($E > 10$ PeV). The 0.785 m^2 Cherenkov telescope is equipped with a 512-pixel SiPM camera, covering $12.8^\circ \times 6.4^\circ$ (Horizontal $\times$ Vertical) field of view. The camera signals are digitized with a 100 MS/s readout system. In this paper, we report the status of the camera development and its performance, and the integration of the telescope.

DOI:10.5506/APhysPolBSupp.15.3-A25

* Presented at the 28$^{\rm th}$ Cracow Epiphany Conference on *Recent Advances in Astroparticle Physics*, Cracow, Poland, 10–14 January, 2022.

1. Introduction

1.1. EUSO-SPB2 mission

Multi-Messenger Astronomy is a rapidly growing field in part due to the observation of gravitational waves with LIGO [1] and the detection of an astrophysical neutrino flux with IceCube [2]. We are working towards opening another Multi-Messenger window to the universe, the Very-High-Energy (VHE) neutrino window (> 10 PeV). The VHE neutrinos can help to understand the most energetic processes in the universe as well as the evolution of astrophysical sources, however, given their small cross section, very few of them have been detected so far. In order to observe them, space-based instruments such as the Probe of Extreme Multi-Messenger Astrophysics (POEMMA) have been proposed [3]. POEMMA is designed to study the flux and composition of the Ultra-High Energy Cosmic Rays (UHECR) above 20 EeV and the flux of VHE neutrinos above 10^7 GeV. POEMMA will be probing the Earth and its atmosphere from the above which gives it the advantage of enormous acceptance compared to the ground-based instruments. A precursor of POEMMA is the Extreme Universe Space Observatory Super Pressure Balloon 2 (EUSO-SPB2), flying at an altitude of 33 km and carrying a Fluorescence Telescope and a Cherenkov Telescope, as shown in figure 1. In this paper, we report on the status of the on-board Cherenkov telescope and discuss its performance.

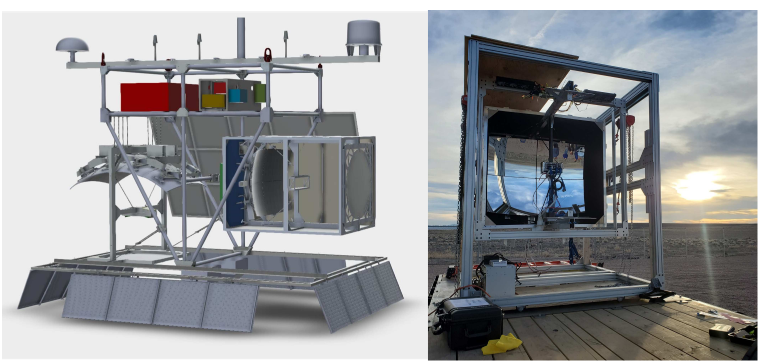

Fig. 1. Left: A rendering of the EUSO-SPB2 payload, with a Fluorescence Telescope pointing down and a Cherenkov Telescope pointing at horizon. Right: A photo of the integrated Cherenkov Telescope during the field test at Delta, Utah.

1.2. Science objectives

The Cherenkov telescope on-board EUSO-SPB2 will probe, for the first time, a volume of 10° above and below the limb of the Earth. When it is pointed above the limb, it will observe the Extensive Air Showers (EAS) initiated by cosmic rays in the upper atmosphere. It is expected that the primary cosmic rays with energies above 1 PeV could result in as many as 100 detected events per hour [4], which will be helpful in evaluating the performance of the telescope. When it is pointed below the limb, it will observe the ambient photon fields, integrated over the Cherenkov telescope's spectral response in order to classify sources of background. Understanding the intensity and variations of the diffused light intensity will be crucial for the space-based instruments such as POEMMA, since it will impact their detection threshold and event reconstruction efficiency. Furthermore, we will use the Earth-skimming technique to search for the VHE-tau neutrinos below the Earth's limb ($E > 10$ PeV). We also intend to perform target of opportunity searches in response to international multi-messenger alerts. The Cherenkov telescope will be capable of rotating towards transient astrophysical sources to search for neutrinos coming from them, although the probability of detecting such events is admittedly very low [5].

2. Cherenkov telescope optics

The Cherenkov telescope optics is based on the Schmidt catadioptric system with a focal length of 860 mm (figure 2, left). The primary mirror is segmented into four identical mirrors with an aperture diameter and area of 1 m and 0.785 m^2, respectively. Throughput is further limited by the Fresnel reflection and absorption from the uncoated PMMA corrector ($\sim 20\%$ loss), 90% reflection of the mirror, and some additional mechanical obscurations. There are two centers of curvature, laterally separated, with the identically aligned mirror segments following a checkerboard pattern: the upper right and lower left mirror segments are aligned to one center of curvature, and the other two mirrors are aligned to another. Given these two different tilts, a parallel light pulse from outside of the telescope produces two spots in the camera with a horizontal offset of 12 mm, or 2 pixels. In this configuration,

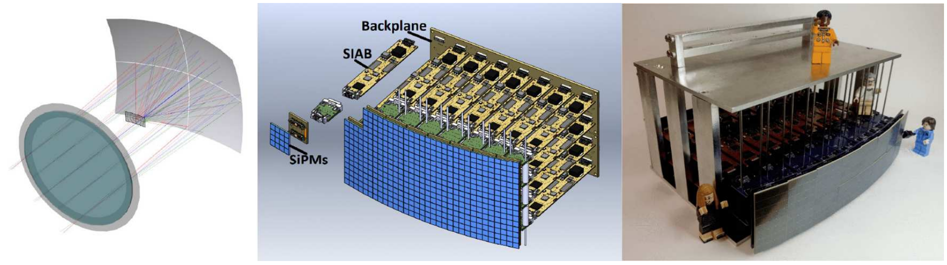

Fig. 2. Left: Schmidt catadioptric optics of the Cherenkov telescope. The mirrors focus the light onto the curved focal plane located between the corrector plate and the mirror. Middle: CAD drawing of the camera. Right: Half assembled camera.

all of the light, geometrically, from a point source at infinity that reflects from the mirror is contained in two 6 mm wide pixels, with their individual RMS spot diameters less than 1.5 mm in diameter.

3. Cherenkov camera instrument

3.1. Silicon photomultiplier

The Cherenkov telescope focal plane is populated with 512-pixel silicon photomultiplier (SiPM) sensors covering an overall field of view of $12.8^\circ \times 6.4^\circ$ in the horizontal and vertical direction, respectively. Each pixel is $6.4\ \text{mm} \times 6.4\ \text{mm}$ wide and they are grouped into a 4×4 matrix. The SiPM matrices are of the S14521-6050AN-04 type from Hamamatsu. The camera includes 32 matrices arranged in an array of 8×4. The SiPM is an electrically and mechanically rugged and highly-sensitive single-photon resolving photo-detector. The chosen SiPM has a broad sensitivity from 200 nm to 1000 nm with a peak photon detection efficiency of 50% at 450 nm. At the operating voltage, direct optical cross-talk is only 1.5% and the temperature dependence of the gain is only $\sim 0.5\%/^\circ\text{C}$.

3.2. Sensor Interface and Amplifier Board (SIAB)

The raw signals from each 4×4 matrix of SiPMs are routed into one Sensor Interface and Amplifier Board (SIAB). A total of 32 SIABs receive power and communication through the backplane, from where the SiPM signals are routed to the digitizer boards (figure 2, right). On the SIAB, SiPM signals are shaped and amplified via two Multipurpose Integrated Circuit (MUSIC) chips. The MUSIC chip is an 8-channel, low-power Application Specific Integrated Circuit (ASIC) designed explicitly for SiPM applications in the Cherenkov telescopes [6]. It provides a 9-bit Digital-to-Analog Converter (DAC) to adjust the SiPM bias voltage and a current-monitor output for each SiPM channel which is being digitized via an Analog-to-Digital Converter (ADC) on-board. A microcontroller on the SIAB (ATMEGA328P) communicates with the MUSIC chips and the ADC via Serial Peripheral Interface (SPI). The microcontroller monitors the current flowing through each SiPM channel, the common bias of the SiPMs, and the temperature of the SiPMs with a thermistor mounted to the back of each SiPM matrix. The temperature measurements will be used offline to correct temperature-dependent gain drifts of the SiPMs.

3.3. Trigger logic

The Cherenkov signal from a typical air-shower induced by Earth-skimming tau-neutrinos illuminates only one pixel in the camera, which will be imaged into two pixels separated by one pixel, due to bi-focal optics. The splitting offset ensures that SiPMs connected to two different MUSIC chips record most of the signal (see the red spots in M1 and M2 in figure 3, middle). The Trigger Board of the Cherenkov camera initiates the readout of the SiPM signals whenever the bi-focal trigger condition is met. This condition requires that two adjacent MUSIC chips record a signal above the threshold of any of their internal leading-edge discriminators. Each MUSIC chip provides a discriminator signal to the input of the Trigger Board. The coincidence logic with a 100 ns coincidence window is formed on the Trigger Board (figure 3, left). The combination of the bi-focal optics and the coincidence trigger reduces the energy threshold by effectively rejecting false triggers due to fluctuations in the Night-Sky-Background (NSB). In addition to the bi-focal trigger, the Trigger Board will run a periodic flasher to illuminate the camera for monitoring the performance of the telescope.

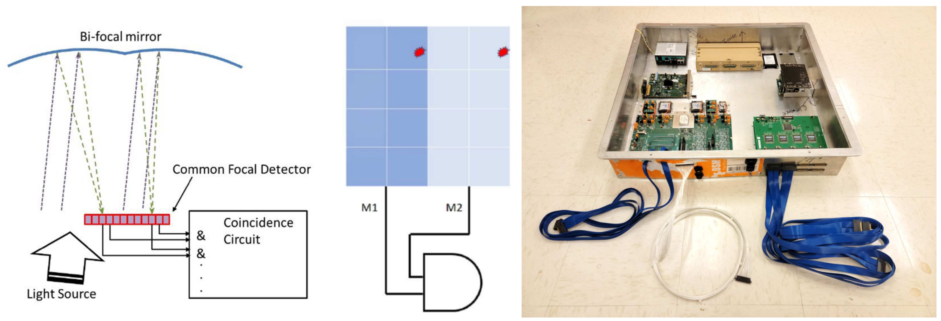

Fig. 3. (Color online) Left and middle: The bi-focal optic duplicates the image and projects it to two locations in the camera. Right: Partially assembled readout electronics.

3.4. Digitization system

The digitization of the shaped SiPM signals is being done via the ASIC Support & Analog-Digital conversion (AsAd) board. The AsAd board was originally developed for the Time-Projection-Chamber (TPC) experiments and has four ASIC for General Electronics for TPC (AGET) chips [7]. Each AGET chip has 64 switched capacitor arrays (SCA), which act as analog ring buffers for the SiPM signal, sampling at a rate of 100 MS/s with a buffer depth of 5.12 μs. We use two AsAd boards to digitize all 512 channels of the camera. Once the readout trigger is issued by the Trigger Board, the SiPM signals stored in the SCAs are digitized with 12-bit resolution. The slow control and communication of AsAd boards with the camera server is managed by a Concentration Board (CoBo). The CoBo is responsible for applying a timestamp, zero suppression, and compression algorithms to the digitized signal. Figure 3, right shows the readout chain including the digitizer boards, CoBo, and CPU.

3.5. Camera server

We are using a dual-core single board computer from RTD Embedded Technologies (CMA24CRD1700HR) for the camera server. This server is responsible for the management and monitoring of the camera components. It uses Ethernet to communicate with the AGET digitizer through the CoBo and the Trigger Board. It uses the System Management Bus (SMBus) to control the front-end electronics (SIAB), serial interface to monitor the housekeeping modules, and CAN bus to control the Power Distribution Unit. Data acquisition starts with the Trigger Board enabling the trigger. Then Trigger Board and CoBo wait for an event to trigger the readout and store the trigger information and digitized SiPM signals into their memory, respectively. Every 5 minutes, the Trigger Board disables the trigger, and the server collects the raw data from the CoBo and Trigger Board memory, and saves them on disk. These raw data are being processed by the event builder and one data stream will be generated. A parallel process generates housekeeping files with information including the SiPM temperatures, bias voltages, currents, and other status data of the camera.

4. Camera performance

4.1. Signal chain linearity

We have evaluated the linearity of the signal chain after the digitization. For this task, we have flashed the SiPM with a picosecond laser with different intensities and digitized the signal amplitude. Figure 4, left shows the time-integrated SiPM signal *versus* the number of detected photons, photoelectrons (PEs). The signal chain is linear up to 300 PEs meeting the required dynamic range. The relative error of the integrated signal compared with the Poisson limit is shown in the middle graph *versus* the number of photoelectrons. Poisson fluctuations in the primary photon signal, which

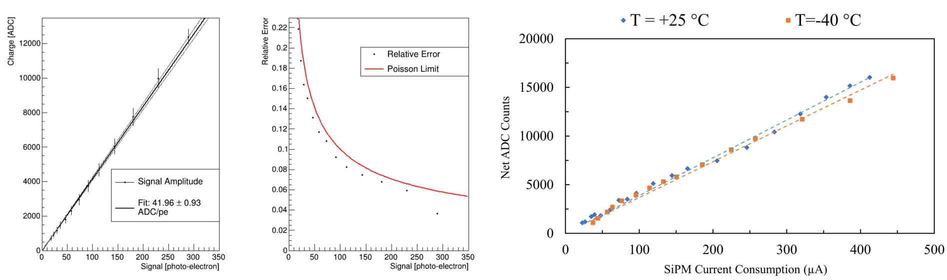

Fig. 4. Left: Linearity and dynamic range of the full signal chain. Middle: Relative error compared with the Poisson limit. Right: Response of the current monitoring.

scale with $1/\sqrt{(\mathrm{PE})}$ dominate the uncertainty in the recorded data. Based on this comparison, the noise characteristics of the signal chain does not seem to be a limiting factor for the performance of the signal chain.

4.2. Current monitoring

The MUSIC chips provide a current output per channel for the purpose of monitoring and protection of the chip against high currents flowing through SiPMs. In order to prevent damaging the input stages of the MUSIC chip, a 24-bit ADC on the SIAB digitizes the current of each of the 16 pixels at a rate of 100 Hz with a resolution of 7.6 μA. The microcontroller continuously monitors this current and automatically turns off a MUSIC channel if the corresponding SiPM current goes above a threshold of 400 μA. The microcontroller attempts to turn the channel back on after waiting for one minute and following a safety protocol to prevent the MUSIC chip from being damaged. Figure 4, right shows the measured current-monitoring response of one channel at room temperature and at $-40°$C.

4.3. Simulation of camera performance

We have studied the bi-focal trigger's performance and reconstruction efficiency of the Cherenkov camera, which is discussed in more detail in [8]. The trigger threshold of the Cherenkov camera is limited by the NSB fluctuations and it increases as the accidental trigger rate goes down. Assuming an NSB intensity of 3.7×10^6 pe/s/mm^2/sr at zenith [9] and taking into account the geometrical effect for observing the limb, the camera's trigger threshold was simulated at different discriminator thresholds, as shown in figure 5, left for a single pixel and the whole camera. With a discriminator

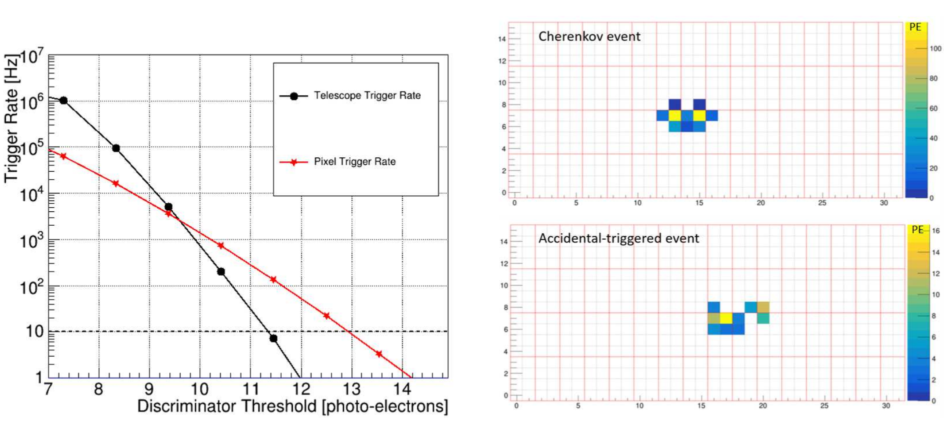

Fig. 5. Left: Simulated trigger rates caused by NSB for a single pixel and the 512-pixel camera after applying the bi-focal trigger. Right: Camera event display of a simulated air-shower event (top) and accidental-triggered event (bottom).

threshold of about 11 photoelectrons, the camera trigger rate after enforcing the coincidence trigger drops below the required 10 Hz not to saturate the data acquisition. The random fluctuations of NSB can trigger the readout as long as two pixels connected to adjacent MUSIC chips receive a signal above the threshold within the coincidence window. An example of such an event alongside a simulated air-shower event is shown in figure 5.

In order to reject accidental triggers, some constraints are applied during the event reconstruction, thus only events that meet the bi-focal requirement would be accepted. With a 10 PEs threshold in the analysis, the algorithm rejects 90% of accidentals and retains 95% of the Cherenkov events if the combined Cherenkov signal is more than 25 PEs, as shown in figure 6, left. The overall reconstruction efficiency in figure 6, right demonstrates that events with more than 50 PEs will be reconstructed with an efficiency of 50% or more. Given that a typical VHE-neutrino event will generate a detectable signal of more than 50 PEs in the EUSO-SPB2 telescope [10], the performance of the Cherenkov telescope is not limited by the camera.

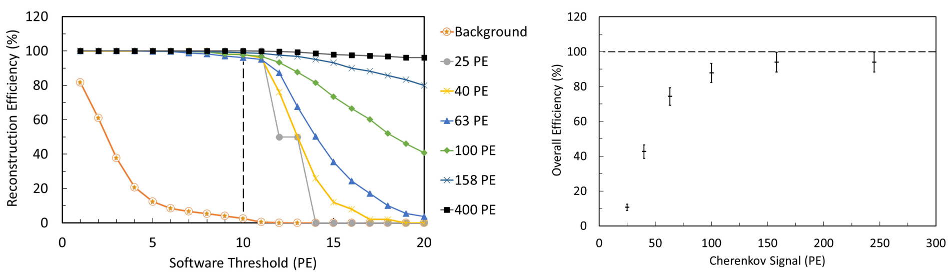

Fig. 6. (Color online) Left: Reconstruction efficiency of the Cherenkov events compared to accidental events (orange stars) for different photoelectron intensities. Right: Combined trigger and reconstruction efficiency of the Cherenkov events as a function of signal intensity.

5. Conclusion

We have developed a Cherenkov telescope that will fly as a part of EUSO-SPB2 balloon flight to study ambient photon field and its fluctuations, and to detect air showers produced by the VHE cosmic rays above-the-limb and the VHE-tau neutrinos below-the-limb. The SiPMs, camera and its electronics are tested and integrated into the telescope, and the field test was completed recently. Data are currently being processed and, at first glance, the results are in line with expectations. The balloon flight is planned to be launched from Wanaka, New Zealand in 2023.

This work was supported by the NASA award 80NSSC19K0627.

REFERENCES

[1] B.P. Abbott *et al.*, «Observation of Gravitational Waves from a Binary Black Hole Merger», *Phys. Rev. Lett.* **116**, 061102 (2016).

[2] IceCube Collaboration (M. Aartsen *et al.*), «Neutrino emission from the direction of the blazar TXS 0506+056 prior to the IceCube-170922A alert», *Science* **361**, 147 (2018).

[3] POEMMA Collaboration (A.V. Olinto *et al.*), «The POEMMA (Probe of Extreme Multi-Messenger Astrophysics) observatory», *J. Cosmol. Astropart. Phys.* **2021**, 007 (2021).

[4] A. Cummings, R. Aloisio, J. Eser, J.F. Krizmanic, «Modeling the optical Cherenkov signals by cosmic ray extensive air showers directly observed from suborbital and orbital altitudes», *Phys. Rev. D* **104**, 063029 (2021).

[5] T.M. Venters *et al.*, «POEMMA's target-of-opportunity sensitivity to cosmic neutrino transient sources», *Phys. Rev. D* **102**, 123013 (2020).

[6] S. Gómez *et al.*, «MUSIC: An 8 channel readout ASIC for SiPM arrays», in: F. Berghmans, A.G. Mignani (Eds.) «SPIE Proceedings Vol. 9899: Optical Sensing and Detection IV», *SPIE*, Washington, USA 2016, pp. 85–94.

[7] E. Pollacco *et al.*, «GET: A generic electronics system for TPCs and nuclear physics instrumentation», *Nucl. Instrum. Methods Phys. Res. A* **887**, 81 (2018).

[8] M. Bagheri *et al.*, «Overview of Cherenkov Telescope on-board EUSO-SPB2 for the Detection of Very-High-Energy Neutrinos», in Proceedings of 37$^{\text{th}}$ International Cosmic Ray Conference (ICRC2021), *PoS* **(ICRC2021)**, 1191 (2021).

[9] C. Benn, S. Ellison, «Brightness of the night sky over La Palma», *New Astron. Rev.* **42**, 503 (1998).

[10] A.L. Cummings, R. Aloisio, J.F. Krizmanic, «Modeling of the tau and muon neutrino-induced optical Cherenkov signals from upward-moving extensive air showers», *Phys. Rev. D* **103**, 043017 (2021).